

# The Implant-supported Telescopic Prosthesis: A Biomechanical Analysis

Håkan Lindström, MSc, Eng Physics<sup>1</sup>/Harold Preiskel, MDS, MSc, FDSRCS<sup>2</sup>

*This in vitro project investigated load transfer through screw-retained telescopic prostheses. Three Brånemark System implants incorporating strain gauges were embedded in an aluminum block. Telescopic prostheses that included 1 mesial and 1 distal cantilever were fabricated over 1 central EsthetiCone and 2 Ti-Adapt abutments. The buffering capacity of the cement in a combined screw-retained/cemented prosthesis was studied. The degree of misfit of the prostheses could be adjusted by applying shims of various thicknesses under the EsthetiCone. Load distribution was measured while a 50-N load was applied in turn over each implant and each cantilever. The results showed that tightening the central prosthetic screw widened the load distribution. The cement accommodated misfits between the layers of the telescope, significantly reducing bending moments on some supporting implants. The system exhibited a degree of tolerance to misfit and can provide a versatile prosthodontic option. (INT J ORAL MAXILLOFAC IMPLANTS 2001;16:34-42)*

**Key words:** *biomechanics, implant abutment, implant-supported prosthesis, load transfer, prosthodontics, telescopic prosthesis*

The telescopic prosthesis is a versatile and successful root-supported dental restoration. With the advent of implant prosthodontics, the telescopic principle was soon adopted and a range of suitable abutments developed. These abutments could be prepared and aligned to a chosen path of insertion, while the emergence profiles and contours of the abutments were under the control of the operator. Furthermore, the esthetics, occlusal surfaces, and structural integrity were not compromised by the need to provide multiple screw access holes. It was even claimed that the grouting effect of the cement might accommodate minor misfits of the casting. Recently, Taylor and coworkers<sup>1</sup> published an excellent review of this background.

Complications, while rare, were not unknown. Accurate seating of the restoration could be difficult. Temporary cements employed to allow for retrievability occasionally washed out, permitting the restoration to break free. On the other hand, and even worse, if an abutment screw loosened or porcelain chipped, it could sometimes be extremely difficult to remove the restoration from the abutment. Therefore, a method was developed to provide the advantages of the telescopic prosthesis with the security and predictable retrievability of the screw-retained prosthesis.<sup>2-4</sup> Each telescopic prosthesis incorporated at least one screw retainer aligned close to the path of insertion. It was felt that the screw component would permit the use of weak temporary cements to facilitate removal, while providing security and assisting with the final seating of the restoration. Initial results showed promise, and a laboratory project was planned to assess whether the design rationale was confirmed in practice.

The aims of this study were: (1) to investigate load transfer and distribution through the supporting components, (2) to examine the significance of the prosthetic screw, and (3) to assess the effects of placing cement between the 3 components of the telescopic abutments. During seating of the casting on its abutments, it is unlikely that all 3 supporting

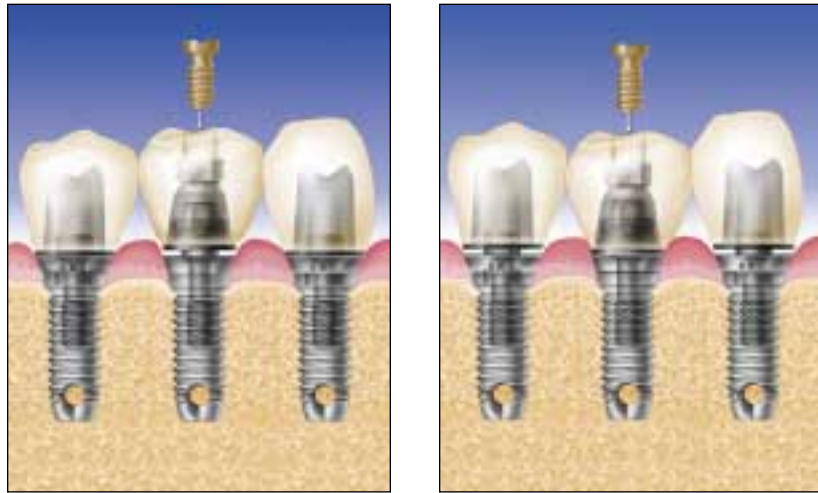
<sup>1</sup>Research and Development Engineer, Nobel Biocare, Göteborg, Sweden.

<sup>2</sup>Consultant in Prosthetic Dentistry, Guy's Hospital, London, England.

**Reprint requests:** Harold Preiskel, Department of Prosthetic Dentistry, Floor 20, Guy's Tower, London Bridge, London SE1 9RT, United Kingdom. Fax: +44 171 486 8337. E-mail: harold.preiskel@lineone.net

**Fig 1a** (Left) Illustration of the “non-buffered” situation, where the 2 telescopic components touch the abutments before the screw retainer.

**Fig 1b** (Right) Illustration of the “buffered” situation, where the screw retainer contacts the abutment before the 2 telescopic components.



units would touch the casting simultaneously. Therefore, 2 geometric possibilities, as well as the transition between them, were examined. The terms *non-buffered situation* (where the 2 telescopic components touched before the screw retainer) and *buffered situation* (where the screw retainer contacted first) were employed (Figs 1a and 1b).

## MATERIALS AND METHODS

### Measurement Rig

Three standard  $13 \times 3.75$ -mm Brånemark System titanium implants (Nobel Biocare, Göteborg, Sweden) were inserted into an aluminum block. The aluminum was drilled and tapped so that the implants could be placed with their long axes parallel to each other. The centers of the implants were separated by 7 mm, according to normal clinical protocol. The implants were placed on the arc of a circle of approximately 15 mm radius to resemble a clinical situation (Fig 2). Before the implants were placed, the 3 external threads closest to the implant head were ground flat to facilitate placement of 3 strain gauges around the periphery at the same height on each implant. The strain gauges were positioned symmetrically, with 120 degrees between them, and projected just above the aluminum block when the implants were placed. The configuration and the computerized analytic equipment enabled the measurement of the strain on 3 sides of the implant.<sup>5</sup> The strains were converted to normal forces and moments as described by Glantz and coworkers,<sup>6</sup> the main difference being that the strain gauges in this study were mounted on the implants instead of the abutments. Briefly, this conversion was made by multiplying each of the 3 mea-

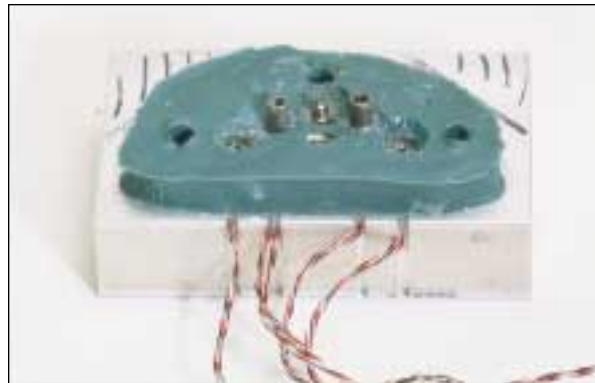


**Fig 2** The in vitro model. Note the different abutments used.

sured strains by a number and then adding the 3 results. The multiplication factors, which were individualized for each strain gauge and implant, were reached via a calibration routine prior to the measurements, during which known forces and moments were applied to the implants.

### Prostheses

A replica of the measurement rig was constructed using standard clinical protocol. Impression copings (Nobel Biocare) were placed over the heads of the 3 implants, and an overall polyether impression (Impregum, Espe, Seefeld, Germany) was made. Implant analogs (Nobel Biocare) were attached to each impression coping, and the impression was cast with a low-expansion artificial stone (Fujirock EP, GC Manufacturing, Leuven, Belgium). Eleven-mm Ti-Adapt abutments (Nobel Biocare) were placed on the mesial and distal implant analogs, and a 1-mm EsthetiCone abutment (Nobel Biocare) was placed



**Figs 3a and 3b** (Left) Uncovered and (right) covered (porcelain-fused-to-metal) prostheses.

on the central analog. Each Ti-Adapt abutment was shortened by approximately 4 mm, but the axial walls were not touched. However, the axial walls were covered with 2-  $\times$  20- $\mu$ m layers of die spacer (Belle de St. Claire, Kerr Manufacturing, Romulus, MI), which ended 1 mm short of the shoulder.

Two castings were made in turn upon these abutments (Figs 3a and 3b), each incorporating 1 mesial and 1 distal cantilevered pontic. The prostheses were waxed, invested, and cast in a platinized gold alloy (Ceramicor, Cendres et Metaux, Biel, Switzerland). An attempt was made to ensure that the dimensions of each casting were similar. Porcelain was fused to one of the castings (Fig 3b), while the other was left uncovered. The prostheses were fabricated in an unbuffered configuration, which enabled the central abutment to be raised in a controlled manner by placing shims of different thicknesses between the implant and the abutment until a buffered situation existed. Shims of 50, 100, and 150  $\mu$ m were produced to fit between the EsthetiCone and its implant analog.

**Load Application.** A loading device, consisting of a weight hanging from a metallic frame above the prosthesis, was constructed. The device applied 50 N axially to the prosthesis in turn to each of the 3 implant positions and to each of the 2 cantilevers. The distribution of the forces was not expected to vary significantly with the magnitude of the applied force. Therefore, the only requirement for the magnitude of the applied force was to result in deformations well above the “noise level” of the system. This was achieved with the 50-N weight.

Although the force in an *in vivo* situation is expected to be applied from different directions, an axial direction was chosen in the present study to best follow the changes in loading distribution introduced by the shims.

**Measurements.** Strain gauge readings were obtained and analyzed as each prosthesis was

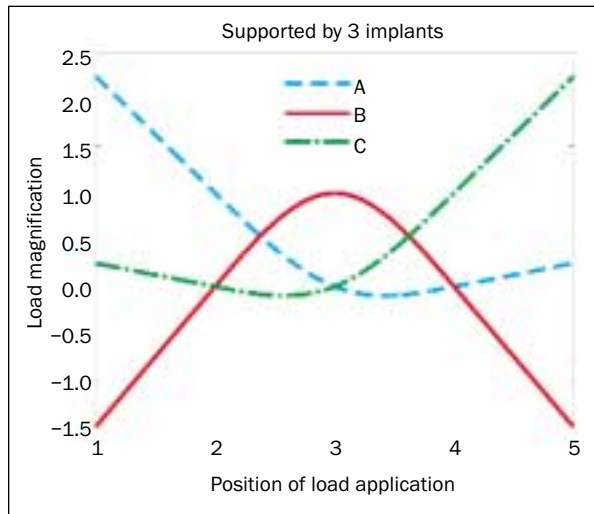
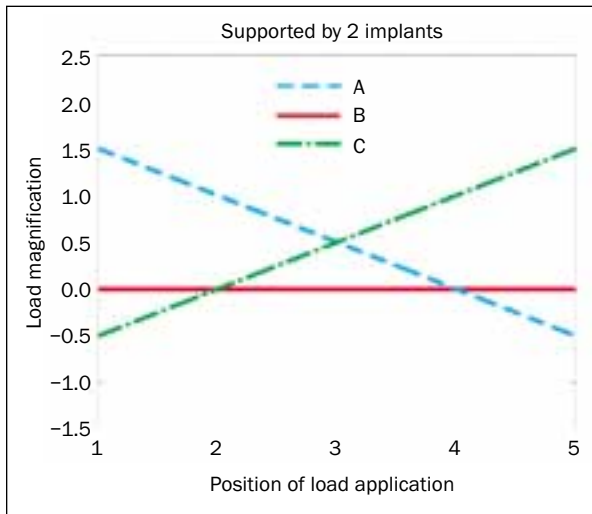
loaded. The initial measurements were made in the unbuffered state, both with and without the gold prosthetic screw attached within the central EsthetiCone abutment. When the gold screw was employed, it was tightened to 10 Ncm using a torque wrench (Tohnichi, Tokyo, Japan). The measurements were then repeated with a temporary cement placed between the 2 sections of the telescopic crowns. Equal amounts of accelerator, base, and modifier were extruded onto a pad and mixed according to the manufacturer’s instructions (Temp Bond, Kerr Manufacturing).

All measurements were repeated employing in turn 50- $\mu$ m, 100- $\mu$ m, and 150- $\mu$ m shims between the EsthetiCone abutment and the underlying implant.

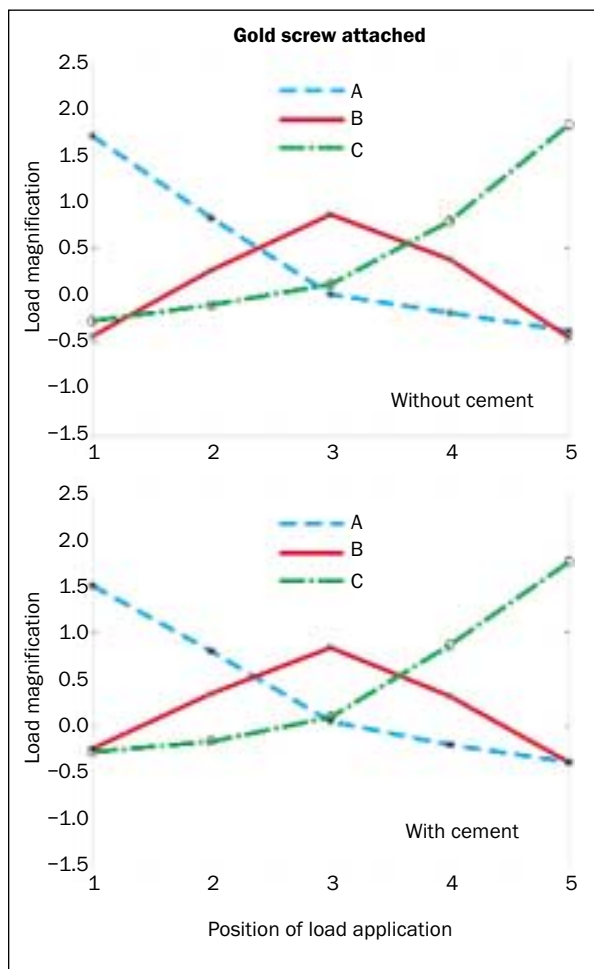
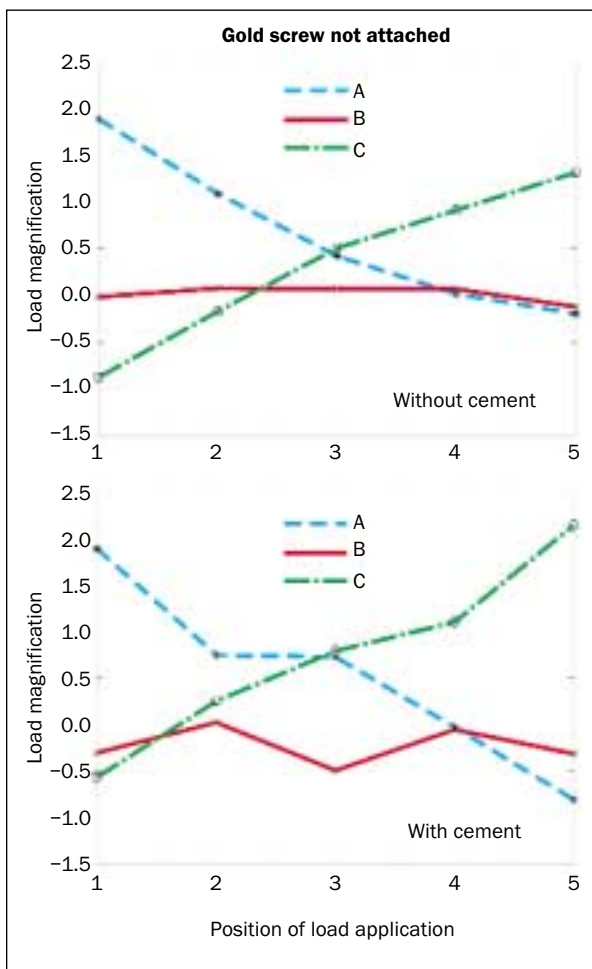
The measuring apparatus allowed the production of an “influence graph”<sup>5,7</sup> that showed how the proportional load was distributed between the supporting implants when it was applied at different positions along the prosthesis. Examples of influence graphs are shown in Figs 4 to 6. The x-axis indicates the position of load application (Fig 7), and the y-axis indicates the proportional amount of load carried by the implant (by definition, positive values indicate compressive forces and negative values indicate lifting forces). Each of the 3 implants is represented by a curve in the graph. It can be seen that in Fig 4b, when load was applied at position 1, then 225% of the applied load was taken by implant A, -150% (a lifting force) by the central implant, B, and 25% by implant C. Amplification of the forces was the result of the lever arm and was considered relatively small.

### Theoretical Model

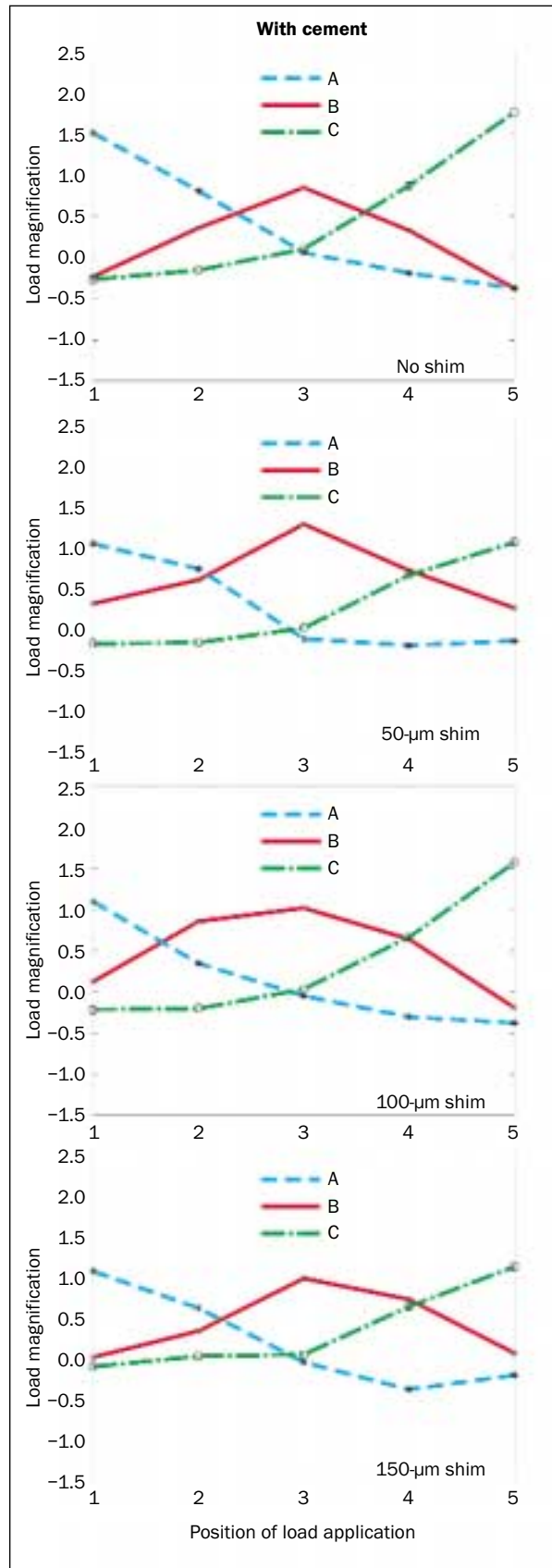
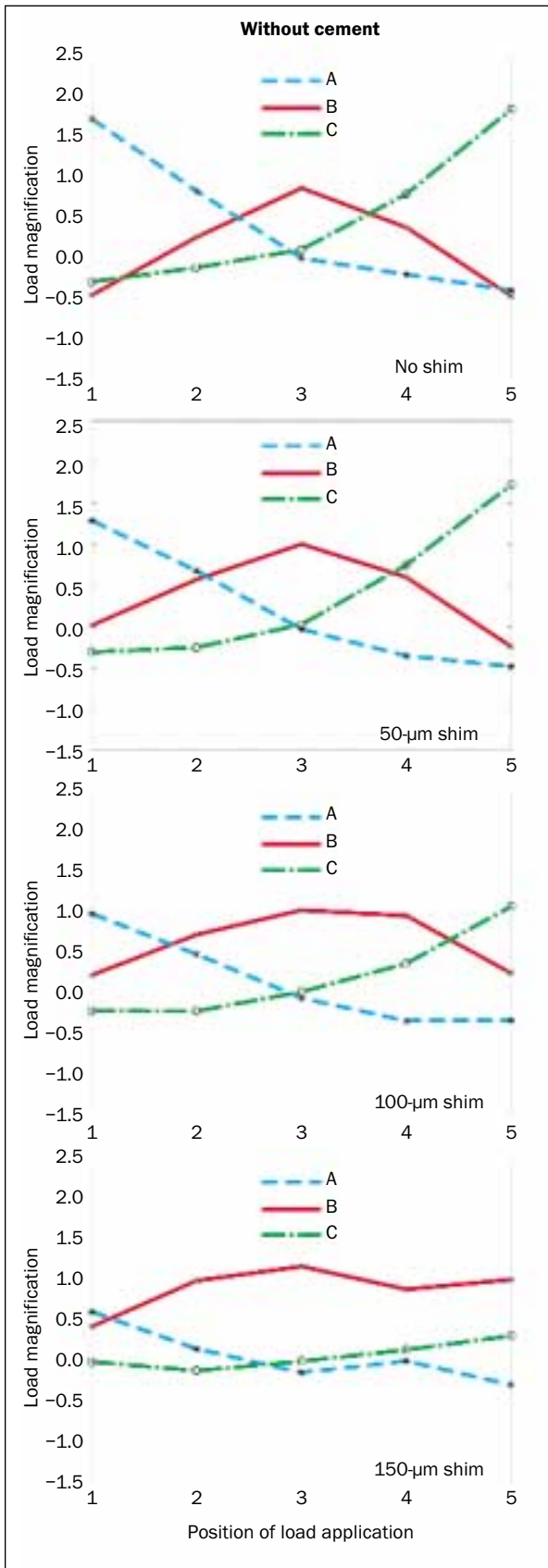
A theoretical model of the measuring arrangement was made using standard engineering methods as, for example, described by Gere and Timoshenko.<sup>7</sup> This model was based on a straight, homogenous beam of uniform cross section resting on 3 supports



**Figs 4a and 4b** Theoretical influence graphs showing the distribution of load between the 3 implants. (Left) Situation in which only the 2 terminal implants are supporting the prosthesis. (Right) The prosthesis is supported by all 3 implants. The position of load application (see Fig 7) is indicated on the x-axis, while the proportion of the load carried is shown on the y-axis. The loads carried by implant A (green), B (red), and C (blue) are shown as separate lines.



**Figs 5a and 5b** Measured influence graphs showing the effect of cement and tightening the gold prosthetic screw on the loading in the prosthesis.



**Figs 6a and 6b** Measured influence graphs illustrating the effects of cement with different shim thicknesses on the loading in the prosthesis. Gold screws were employed in all cases.

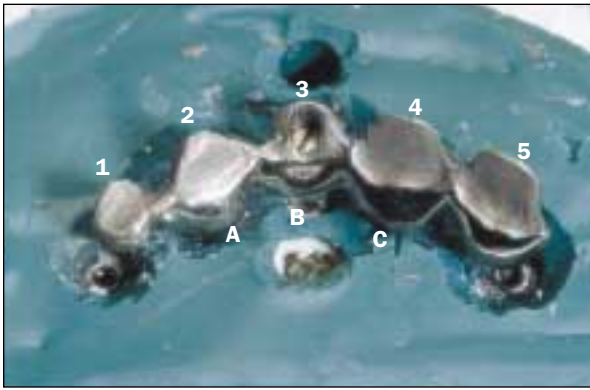
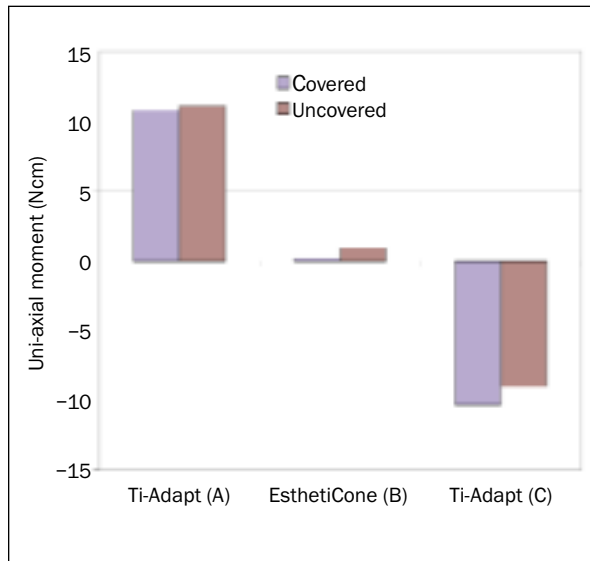


**Fig 7** (Above) Illustration demonstrating load application points and implant positions.

**Fig 8** (Right) Moments induced by seating the castings with no screw attached. The results of the covered (ie, PFM) and uncovered castings were very similar.



at right angles to the long axis of the beam. From this model, a theoretical influence graph was calculated wherein the prosthesis was ideally supported by either the 2 distal implants or all 3 implants (Figs 4a and 4b). This model will predict axial forces at the supports, but not bending moments. Calculations with more refined models, including bending moments and implant flexibility,<sup>8</sup> have shown that this simpler approach is often sufficient for estimations of force distribution.

## RESULTS

The influence graphs and preload data obtained with the porcelain-fused-to-metal (PFM) prosthesis and with the uncovered restoration were similar (Fig 8); therefore, this report will focus on the results from the uncovered casting only.

Figures 5a and 5b show the measurement with the uncovered prosthesis with no shim attached. A comparison of these graphs with the theoretical graphs in Figs 4a and 4b reveals that the general features of the measured graph with no screw attached were the same as those of the theoretical graph supported by 2 implants. When the screw was inserted, the graph resembled the theoretical graph supported by 3 implants. There was no difference between corresponding cemented and non-cemented samples.

Figures 6a and 6b show the effects of placing shims under the central abutment. Similar results were found with no shim and with a 50- $\mu$ m shim in the cemented and non-cemented situations. Both

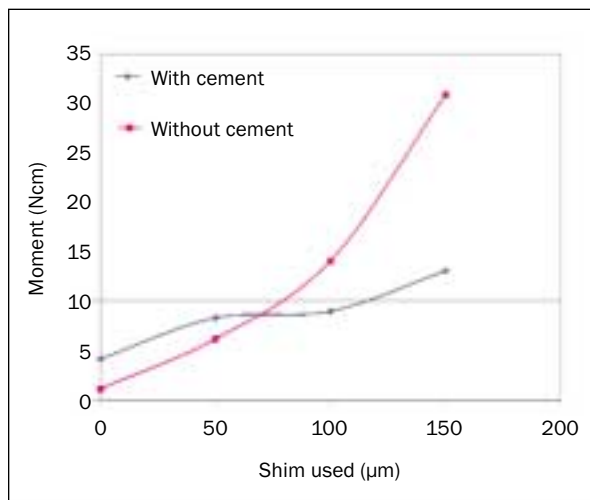
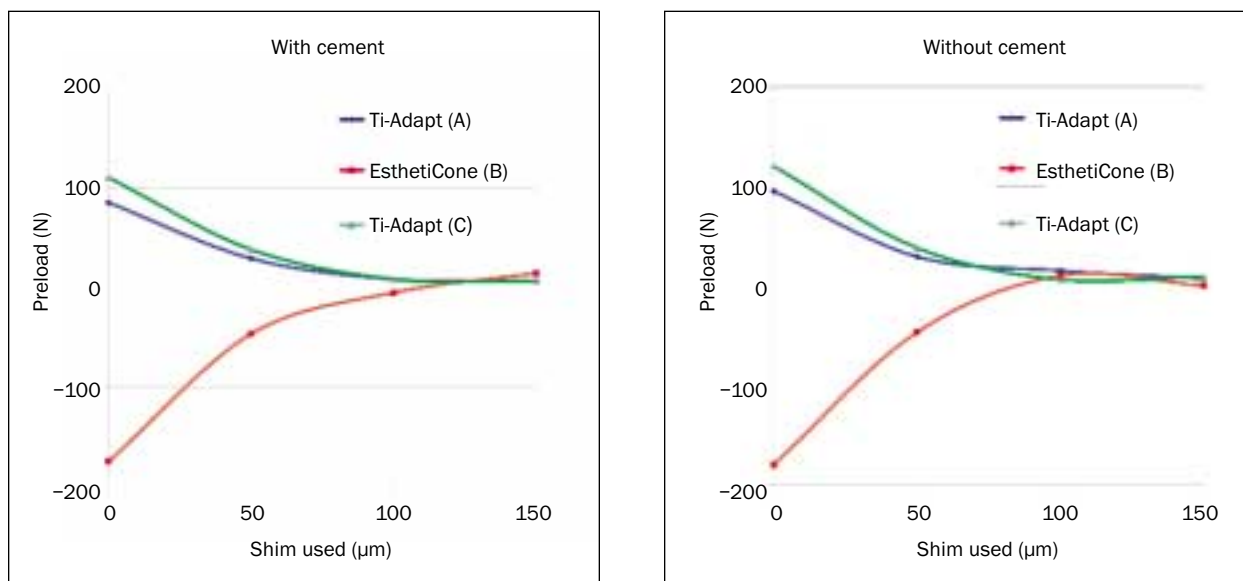


**Fig 9** Moments in the central implant when the load was applied in position #5.

showed the same general features as the influence graph supported by 3 implants (Fig 4b). The features of the influence graphs in Fig 6 started to change in the non-cemented situation when a 100- $\mu$ m shim was used and were changed still further when the 150- $\mu$ m shim was substituted. Where cement was employed, there were no significant changes in the influence graphs with any of the shim thicknesses used.

Figure 9 illustrates the bending moment in the central implant as load was applied to a cantilevered extension (position 5). The graph shows the magnitude of the bending moment when different shims



**Figs 10a and 10b** Effect of different shim thickness on the preload within each implant, either with cement (*left*) or without cement (*right*).

were used, which changed the prosthesis from a non-buffered into a buffered configuration. Cemented and uncemented restorations produced similar results with the smallest shim. However, the 150- $\mu\text{m}$  shim produced more than a twofold magnification of bending moment in the non-cemented situation when compared with the cemented configuration.

Figures 10a and 10b show the effect of the shim on the preload<sup>9</sup> for the cemented and non-cemented situation. When no shim was used, there was a lifting force in the central screw-retained unit of 200 N. This force was compensated by compressive forces of 100 N on each of the 2 adjacent implants, resulting in a net force of 0 N acting on the structure. As the central abutment was raised by introducing shims, the magnitude of these forces was reduced until they were zero when a 100- $\mu\text{m}$  shim was employed, as was the case for the 150- $\mu\text{m}$  shim. No difference was observed between the cemented and non-cemented situations.

## DISCUSSION

The results obtained from the strain gauge analysis on the implants were similar to those that might be expected using a theoretical model. The strain gauge signals were stable, and the results suggest a sound method of measurement. Similar figures were

produced by the PFM prosthesis and by the gold casting without porcelain (Fig 8). This implies that while the application of porcelain may have caused some dimensional change and increased the stiffness of the prosthesis, the effects were insignificant. Restorations of larger spans or different geometry may well behave in a different manner.<sup>10,11</sup>

Figures 5a and 5b show that without a shim and without the gold prosthetic screw, the prosthesis was supported by only the 2 Ti-Adapt abutments. Tightening the gold screw changed the load distribution pattern into one that resembled the theoretical graph in which the prosthesis was supported by 3 implants (Fig 4b). This suggests that the preload in the gold screw was sufficient to deform the prosthesis so that the structure was supported by all 3 implants. This situation provides a favorable distribution of load with relatively low load amplification factors.<sup>5,9</sup> In no case did the addition of cement make any difference in the load distribution.

Deformation of the prosthesis resulted in a static preload within the entire implant/prosthesis structure, which registered as a 200-N lifting force in the central implant counteracted by compressive forces of 100 N in each of the adjacent implants (Figs 10a and 10b). The zero net force on the structure is an illustration of Newton's first law. The measured forces are in agreement with previous *in vitro* studies.<sup>12</sup> Placement of a 50- $\mu\text{m}$  shim under the central

EsthetiCone unit produced a decrease in the registered preload forces but no difference in their relative magnitude (Fig 10). It appears that the degree of misfit over the central EsthetiCone was reduced by introducing the shim; hence, less force was required to close the smaller gap. When the thicker shim of 100- $\mu\text{m}$  was used, the preloads were reduced to zero, since the prosthesis no longer needed to be deformed to allow for the tightening of the screw. However, this does not necessarily mean that there was a perfect "passive fit" on all 3 supporting abutments. In a buffered situation, the prosthesis need not deform to attach the screw, although a buffered situation cannot be regarded as a passive fit. Hence, the internal preload forces in a buffered situation are believed to be zero, as opposed to a non-buffered situation, where the prosthesis was deformed when the screw was tightened. From this it is concluded that the misfit above the EsthetiCone was between 50  $\mu\text{m}$  and 100  $\mu\text{m}$ , since this is the range where the preloads reached zero and the configuration changed from non-buffered to buffered. This degree of misfit is within what is reported to be common in a clinical situation.<sup>13,14</sup> The preloads of the system were not affected by the application of cement.

To compensate for the misfit, static forces are introduced within the prosthesis. Clinical studies<sup>15</sup> have indicated that forces and strains caused by misfits on the order of 100  $\mu\text{m}$  can be tolerated by bone without a progressive loss of marginal bone. This is in contrast to dynamic or single-cycle forces or strains, which are believed by some authors<sup>16-18</sup> to trigger unfavorable biologic responses, although the exact effect of large dynamic strains on bone is still not known.<sup>19,20</sup>

The load distribution with shims placed under the central EsthetiCone can be seen in Figs 6a and 6b. With no shim or a 50- $\mu\text{m}$  shim under the EsthetiCone, the prosthesis was supported by all 3 implants. Further increases in the height of the EsthetiCone produced a buffered configuration, as the Ti-Adapts were no longer in unforced contact with the prosthesis. This change in the influence graph was observed in the non-cemented case going from the 50- $\mu\text{m}$  shim to the 100- $\mu\text{m}$  shim and was marked when the 150- $\mu\text{m}$  shim was employed. Hence, the transition from a buffered to a non-buffered configuration took place somewhere between 50  $\mu\text{m}$  and 100  $\mu\text{m}$ , which corresponds to the previous estimate. However, this change was not apparent in cemented measurements, indicating that although the Ti-Adapts and prosthesis were no longer in contact, the cement acted as a buffer, restoring a 3-implant load distribution pattern to the buffered situation.

When a force was applied to the end of the buffered prosthesis, the prosthesis appeared to deform until the nearest Ti-Adapt made contact with it. Before this contact was made, the applied force caused a large bending moment in the central implant. This specific situation and the transition from an unbuffered into a buffered configuration using different shims is studied in Fig 9. Here it can be seen that the moment in the central implant in a buffered situation without cement was more than twice that of the cemented prosthesis. This is related to the buffering capacity of the cement. In a clinical situation, numerous chewing cycles will repeatedly expose a prosthesis to deformation. With cement in place, the bending moment in the central implant of each cycle will be halved, which should decrease the risk of fatigue fracture.<sup>17,21</sup>

The differences between the theoretical curves and the present results may be explained by differences between the situations. The theoretical model is based on a straight, homogenous bar of uniform, rectangular cross-section that is rigidly supported in both tension and compression and is permitted to rotate around only 1 axis. However, since the interest here is in comparing general features, these differences are believed to play a minor role.

The aluminum block in which the implants were embedded did not possess the same physical properties as bone; thus, caution must be used in extrapolating the results into clinical practice. Nevertheless, the combined cemented/screw-retained system appears to provide the operator with a degree of tolerance of the small misfits that occur in a clinical environment, where one might be unaware of a buffered or non-buffered situation. Furthermore, tightening of the screw assisted with the seating of the prosthesis. Placement of cement between sections of the telescope would seem prudent for load transfer, in addition to retention, or to act as a seal, although the potential hazards of leaving excess cement beneath the mucosa are appreciated. It might be speculated that the degree of tolerance provided by the system may become particularly useful for immediate loading techniques. However, what appears clear is that the results of this project are encouraging. When viewed with previous clinical data, the concept is worthy of further development.

## CONCLUSIONS

1. A telescopic prosthesis supported by the abutments at both ends only was termed *unbuffered*. In this situation, tightening the central prosthetic

screw to 10 Ncm caused the prosthesis to rest on all 3 implants, resulting in an enhanced load distribution.

2. The greater the misfit, the larger the magnitude of the involved forces when the prosthetic gold screw was tightened.
3. Without cement, there was a significant difference in the load distribution patterns between a buffered and non-buffered configuration. When cement was applied, the difference was eliminated.
4. Placement of cement in a buffered situation can reduce the bending moment in the central implant by half. This might decrease the risk of fatigue fracture.
5. In non-buffered configurations, no differences were seen with the addition of cement.

Hence, the combined screw-retained telescope offers tolerance that could be valuable in clinical practice. It also offers ease of maintenance, design versatility, and security against accidental dislodgement.

## ACKNOWLEDGMENT

The authors acknowledge the valuable contributions by Dr Tomas Lindh, Umeå, Sweden, and Mr Tomas Bäck, Nobel Biocare, for valuable help in constructing the measurement rig. We also appreciate the advice received from Dr Bo Rangert of Nobel Biocare. We express our thanks to Mr J. Elias for his skilled technical work and to Ms Gillian Lee for her assistance with the illustrations.

## REFERENCES

1. Taylor TD, Agar JR, Vogiatzi T. Implant prosthodontics: Current perspective and future directions. *Int J Oral Maxillofac Implants* 2000;15:66–75.
2. Preiskel HW, Tsolka P. The DIA anatomic abutment system and telescopic prostheses: A clinical report. *Int J Oral Maxillofac Implants* 1997;12:628–633.
3. Preiskel HW, Tsolka P. The implant in prosthodontics today—A personal viewpoint. *Br Dent J* 1997;182(6):202–205.
4. Preiskel HW. Telescopic prostheses. *Int J Oral Maxillofac Implants* 1998;13:352–357.
5. Lindström H. In-Vivo Strain-Gauge Measurement of Load on the Abutment of a Brånemark Dental Implant [thesis]. Göteborg: Chalmers Univ of Technology, 1998.
6. Glantz P-O, Rangert B, Svensson A, Stafford GD, Arnvidarsson B, Randow K, et al. On clinical loading of osseointegrated implants. *Clin Oral Implants Res* 1993;4:99–105.
7. Gere JM, Timoshenko SP. *Mechanics of Materials*, SI ed 3. London: Chapman & Hall, 1991.
8. Daellenbach K, Hurley E, Brunski JB, Rangert B. Biomechanics of in-line vs. offset implants supporting a partial prosthesis [abstract #1327]. *J Dent Res* 1996;75(special issue):183.
9. Rangert B, Jemt T, Jörneus L. Forces and moments on Brånemark implants. *Int J Oral Maxillofac Implants* 1989;4:241–247.
10. Davis DM, Rimrott R, Zarb GA. Studies on frameworks for osseointegrated prostheses. Part 2. The effect of adding acrylic resin or porcelain to form the occlusal superstructure. *Int J Oral Maxillofac Implants* 1988;3:275–280.
11. Korioto TW, Johann AR. Influence of mandibular superstructure shape on implant stresses during simulated posterior biting. *J Prosthet Dent* 1999;82(1):67–72.
12. Smedberg J-I, Nilner K, Rangert B, Svensson S-A, Glantz P-O. On the influence of superstructure connection on implant preload: A methodological and clinical study. *Clin Oral Implants Res* 1996;7:55–63.
13. Jemt T, Lie A. Accuracy of implant-supported prostheses in the edentulous jaw. Analysis of precision of fit between cast gold-alloy framework and master casts by means of a three-dimensional photogrammetric technique. *Clin Oral Implants Res* 1995;6:172–180.
14. Jemt T. In vivo measurement of precision of fit involving implant-supported prostheses in the edentulous jaw. *Int J Oral Maxillofac Implants* 1996;11:151–158.
15. Jemt T, Book K. Prosthesis misfit and marginal bone loss in edentulous implant patients. *Int J Oral Maxillofac Implants* 1996;11:620–625.
16. Van Steenberghe D, Jacobs R. Physiological aspects of implant-supported prostheses. In: Worthington P, Brånemark P-I (eds). *Advanced Osseointegration Surgery: Applications in the Maxillofacial Region*. Chicago: Quintessence, 1992:40–46.
17. Rangert B, Krogh PHJ, Langer B, van Roekel N. Bending overload and implant fracture: A retrospective clinical analysis. *Int J Oral Maxillofac Implants* 1995;10:326–334.
18. Quirynen M, Naert I, van Steenberghe D. Fixture design and overload influence marginal bone loss and fixture success in the Brånemark System. *Clin Oral Implants Res* 1992;3:104–111.
19. Brunski JB. Biomechanical factors affecting the bone-dental implant interface. *Clin Mater* 1992;10:153–201.
20. Brunski JB, Puleo D, Nanci A. Biomaterials and biomechanics of oral and maxillofacial implants: Current status and future development. *Int J Oral Maxillofac Implants* 2000;15:15–46.
21. Rangert B, Forsmalm G. Strength characteristics of CP titanium. *Nobelpharma News* 1994;8(1):7.